Accepted Manuscript

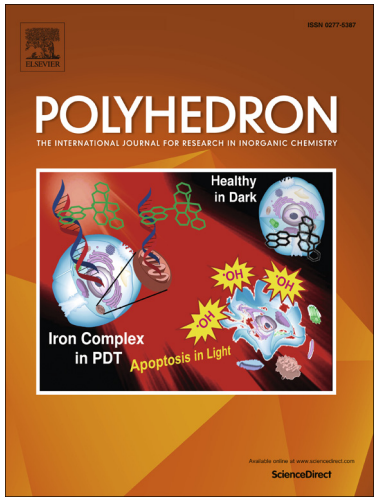

Doubly phenoxo-bridged M-Na (M = Cu(II), Ni(II)) complexes of tetradentate Schiff base: Structure, photoluminescence, EPR, electrochemical studies and DFT computation

Kuheli Das, Amitabha Datta, Suman Roy, Jack K. Clegg, Eugenio Garribba, Chittaranjan Sinha, Hulya Kara

PII: S0277-5387(14)00243-5
DOI: http://dx.doi.org/10.1016/j.poly.2014.04.032
Reference: POLY 10676

To appear in: *Polyhedron*

Received Date: 3 January 2014
Accepted Date: 11 April 2014

Please cite this article as: K. Das, A. Datta, S. Roy, J.K. Clegg, E. Garribba, C. Sinha, H. Kara, Doubly phenoxo-bridged M-Na (M = Cu(II), Ni(II)) complexes of tetradentate Schiff base: Structure, photoluminescence, EPR, electrochemical studies and DFT computation, *Polyhedron* (2014), doi: http://dx.doi.org/10.1016/j.poly.2014.04.032

Doubly phenoxo-bridged M-Na (M = Cu(II), Ni(II)) complexes of tetradentate Schiff base: Structure, photoluminescence, EPR, electrochemical studies and DFT computation

Kuheli Das[a], Amitabha Datta[b,*] Suman Roy[a], Jack K. Clegg[c], Eugenio Garribba[d], Chittaranjan Sinha[a,*] Hulya Kara[b]

[a]*Department of Chemistry, Inorganic Chemistry Section, Jadavpur University, Kolkata - 700032, India*

[b]*Fizik Bölümü, Fen-Edebiyat Fakültesi, Balikesir Üniversitesi, Balikesir - 10100, Türkiye*

[c]*School of Chemistry and Molecular Biosciences, The University of Queensland, Brisbane St Lucia, QLD 4072, Australia*

[d]*Dipartimento di Chimica e Farmacia and Centro Interdisciplinare per lo Sviluppo della Ricerca Biotecnologica e per lo Studio della Biodiversità della Sardegna, Università di Sassari, Via Vienna 2, I-07100 Sassari, Italy*

---

* Corresponding author. Fax: 91-33-2413-7121.

E-mail addresses: c_r_sinha@yahoo.com (C.R. Sinha); amitd_ju@yahoo.co.in (A. Datta)

A B S T R A C T

Phenoxo-bridged complexes [M(μ-L)Na(ClO_4)(CH_3OH)] (M = Cu(II) (**1**) and Ni(II) (**2**)) (H_2L = *N*,*N*'-Bis(3-methoxysalicylidenimino)-1,3-diaminopropane, C_6H_3(OMe)(OH)–CH=N–$(CH_2)_3$–N=CH–C_6H_3(OMe)(OH)) are structurally characterised by single-crystal X-ray diffraction study. M(II) appears in the square-plane geometry with MN_2O_2 coordination sphere, while the sodium ion exists with NaO_6 distorted octahedral environment. The molecules pack in the solid-state forming three-dimensional arrays through C-H---O, O-H---O, C-H---π, and π---π interactions. The spectral and redox properties are theoretically explained by DFT computation of optimised geometry of the complexes.

Keywords: Schiff base, Cu(II) and Ni(II) complexes, EPR, Cyclic voltammetry, Photoluminescence

1. Introduction

Metal complexes incorporating different N,O donor ligands have received considerable attention due to their ability to bind different cations [1], anions [2,3], and neutral compounds [4-7]. The choice of ligands encoding some degree of flexibility is an important factor in the design of metal-ligand complexes of different nuclearity, dimensionality, redox ability, chirality etc. which illustrates a range of applications in catalysis [8,9], selective host-guest recognition [10-13] and use as building blocks in the formation of extended structures [14,15]. The chemistry of Schiff base ligands has received continuous and intensive attention in many fields of research because of their unique coordination and structural properties. Metal-salicylaldimines with *o*-phenoxo group(s) are fascinating ligands that can coordinate with not only p- and d-block metal elements but also alkali-metal ions. Hetero-binuclear complexes of alkali- and transition metal-salicylaldimines are useful molecules in small-molecule activation [16], electron storage [17], and they carry polar organometallics [18].

Ligands based on mixed donor Schiff bases have been used for the formation of hetero-metallic complexes [19-21]. The phenoxy bridging tetradentate N_2O_2 ligand is a compartmental system [22-25], sometime forms coordinatively unsaturated metal centers [26-29] allowing for their incorporation into coordination polymers [30-32]. *N*,*N*'-Bis(3-methoxysalicylidenimino)-1,3-diaminopropane (H_2L) has been used by us to prepare heterometallic 3d/4f [28,33-37], 3d/3d [28,38,39] and 3d/alkali metal complexes [28,40,41]. It is reported that some copper(II)-sodium(I) and nickel(II)-sodium(I) complexes with salen-type compartments Schiff bases [42-44] where structural determination has revealed that the transition metal ions are placed in the N_2O_2 compartment of the ligand, and sodium(I) is placed in the O_4 compartment of

the complexes. In the extension to these studies, herein we report spectroscopic studies (IR, UV-Vis, Fluorescence), X-ray structures, EPR, electrochemical measurements and DFT calculations, of two heterometallic complexes, [Cu(μ-L)Na(ClO_4)(CH_3OH)] (**1**) and [Ni(μ-L)Na(ClO_4)(CH_3OH)] (**2**). To the best of our knowledge no measurements of their EPR spectra or DFT calculations of these complexes have emerged in the literature.

2. Experimental

2.1. Materials

o-Vanillin and 1,3-diaminopropane (Merck, India), nickel perchlorate hexahydrate, copper perchlorate hexahydrate and sodium perchlorate (Sigma-Aldrich) were purchased and used as received without further purification. All solvents used were of reagent grade. The ligand (H_2L) synthesis was carried out following the published procedure [45].

2.2. Physical techniques

Elemental analyses were performed on a Heraeus CHN-OS Rapid Elemental Analyzer at the Instrument Centre of the NCHU. Infrared spectra were recorded on a Perkin-Elmer 883-Infrared spectrophotometer in the range 4000–400 cm^{-1} as KBr pellets. Electronic spectra were measured on a Hitachi U 3400 (UV–Vis–NIR) spectrophotometer in methanol. EPR spectra were recorded from 0 to 10000 Gauss in the temperature range 77-298 K with an X-band (9.15 GHz) Varian E-9 spectrometer. The EPR parameters reported in the text were obtained by simulating the spectra with the computer program Bruker WinEPR SimFonia [46]. In all the simulations, second-order effects were taken into account, the ratio Lorentzian/Gaussian, affecting the line

shape, was set to 1 and the line width used for *x*, *y*, *z* axes was 22, 25 and 30 Gauss, respectively. Emission spectra were examined by LS 55 Perkin–Elmer spectrofluorimeter at room temperature (298 K) in CH_3CN solution under degassed condition. The fluorescence quantum yield of the complexes was determined using carbazole as a reference with known Φ_R of 0.42 in MeCN [47]. The complex and the reference dye were excited at same wavelength, maintaining nearly equal absorbance (~0.1), and the emission spectra were recorded. The area of the emission spectrum was integrated using the software available in the instrument and the quantum yield is

$$\phi_s / \phi_R = \left[A_S / A_R \right] \times \left[(Abs)_R / (Abs)_S \right] \times \left[\eta_S^2 / \eta_R^2 \right]$$

Here, Φ_S and Φ_R are the fluorescence quantum yield of the sample and reference, respectively. A_S and A_R are the area under the fluorescence spectra of the sample and the reference, respectively, $(Abs)_S$ and $(Abs)_R$ are the respective optical densities of the sample and the reference solution at the wavelength of excitation, and η_S and η_R are the values of refractive index for the respective solvent used for the sample and reference. Electrochemical measurements were performed using computer-controlled CH-Instruments, Electrochemical workstation, Model No CHI 600D (SPL) with Pt-disk electrodes. All measurements were carried out under nitrogen environment at 298 K with reference to SCE electrode in acetonitrile using [*n*-Bu_4N]ClO_4 as supporting electrolyte. The reported potentials are uncorrected for junction potential.

2.3. Synthesis of the complexes

2.3.1. Preparation of complex [Cu(μ-L)Na(ClO_4)(CH_3OH)] (**1**)

Upon addition of H_2L (0.34 g, 1 mmol) in methanol (20 mL) to $Cu(ClO_4)_2 \cdot 6H_2O$ (0.37 g, 1 mmol) in the same solvent the mixture was stirred for half

an hour and then a solution of $NaClO_4$ (0.12 g, 1 mmol) in the minimum volume of water was added, and the reaction mixture was kept undisturbed and allowed to evaporate slowly. After ten days, dark brown coloured, rectangular-shaped single crystals of **1** were obtained. The crystals were filtered off, washed with water and dried in air. Yield: 71% (0.39 g). Anal. Calc. for $C_{20}H_{24}NaCuN_2O_9Cl$: C, 43.02; H, 4.33; N, 5.02. Found: C, 42.83; H, 4.41; N, 5.18%.

2.3.2. Preparation of complex [Ni(μ-L)Na(ClO_4)(CH_3OH)] (**2**)

Upon addition of H_2L (0.34 g, 1 mmol) in methanol (20 mL) to $Ni(ClO_4)_2 \cdot 6H_2O$ (0.36 g, 1 mmol) in the same solvent produced instantly a green solution. The mixture was stirred for half an hour and then a solution of $NaClO_4$ (0.12 g, 1 mmol) in the minimum volume of water was added, and the reaction mixture was kept undisturbed and allowed to evaporate slowly. After ten days, dark-green, rectangular-shaped single crystals of **2** were obtained. The crystals were filtered off, washed with water and dried in air. Yield: 68% (0.38 g). Anal. Calc. For $C_{20}H_{24}NaNiN_2O_9Cl$: C, 43.40; H, 4.37; N, 5.06. Found: C, 43.58; H, 4.48; N, 4.92%.

2.4. X-Ray crystallography

The crystals [Cu(μ-L)Na(ClO_4)(CH_3OH)] (**1**) (0.41 × 0.17 × 0.12 mm) and [Ni(μ-L)Na(ClO_4)(CH_3OH)] (**2**) (0.30 × 0.30 × 0.20 mm) were used for data collection. The Oxford Gemini Ultra employing confocal mirror monochromated Cu-K_α radiation generated from a sealed tube (λ 1.54184 Å) used for data collection of **1** and graphite monochromated Mo-K_α radiation generated from a sealed tube (λ 0.71073 Å) was used for **2** with ω and ψ scans at 120(2) K. Data integration and reduction were undertaken with CrysAlisPro [48] and subsequent computations were

carried out using the WinGX-32 graphical user interface [49]. Gaussian and empirical absorption corrections were applied using CryAlisPro [48] in the hkl range $-17 \leq h \leq 20$, $-9 \leq k \leq 9$; $-23 \leq l \leq 21$ for **1** and $-10 \leq h \leq 10$, $-20 \leq k \leq 19$; $-32 \leq l \leq 31$ for **2** in the θ range 3.24-72.02° for **1** and 2.98-30.82° for **2**. Structures were solved by direct methods using SHELXS-97 [50], then refined and extended with SHELXL-97 [50]. Carbon-bound hydrogen atoms were included in idealized positions and refined using a riding model. Oxygen-bound hydrogen atoms were first located in the difference Fourier map before refinement with bond length and angle restraints. Compound **2** crystallizes with two molecules in the asymmetric unit. One of the oxygen atoms from the Cl(1) containing perchlorate anion shows disorder over two positions with occupancies of 0.6 and 0.4. These atoms were modeled with equal thermal parameters. The propylene section of **1** is disordered and was modeled over two equal occupancy positions. Each individual pair of disordered atoms was also included with equal thermal parameters. The perchlorate anion was also disordered and modeled over two 50 % occupancy positions. Crystallographic data is summarized in **Table 1**.

2.5. Theoretical Calculations

Full geometry optimization of **1** and **2** were carried out using density functional theory (DFT) at the B3LYP level [51]. All calculations were performed using the Gaussian 03 program package [52] with the aid of the Gauss View visualization program [53]. For C, H, N, O, and Cl the 6-31G(d) basis set were assigned, while for Cu and Ni the LanL2DZ basis set with effective core potential were employed [54]. The vibrational frequency calculations were performed to ensure that the optimized geometries represent the local minima and there are only positive eigen values. Vertical electronic excitations based on B3LYP optimized geometries

were computed using the time-dependent density functional theory (TD-DFT) formalism [55-57] in acetonitrile using conductor-like polarizable continuum model (CPCM) [58]. Gauss Sum was used to calculate the fractional contributions of various groups to each molecular orbital [59].

3. Results and discussion

3.1. Syntheses and formulation

The ligand, H_2L (*N*,*N*'-Bis(3-methoxysalicylidenimino)-1,3-diaminopropane), is prepared by the condensation of *o*-vanillin and 1,3-diaminopropane (1:2 mole ratio) in methanol, following the literature method [45]. H_2L is then reacted with $M(ClO_4)_2 \cdot 6H_2O$ in methanol followed by the addition of $NaClO_4$ with 1:1:1 ratio and the complexes of composition, $[M(\mu\text{-}L)Na(ClO_4)(CH_3OH)]$ (M = Cu(II) (**1**) and Ni(II) (**2**)) are crystallized by slow evaporation of the solvent.

The IR spectra of the complexes (**1** and **2**) show ν(C–O) band at 1230 cm^{-1} and 1244 cm^{-1} for **1** and **2**, respectively corresponding to the deprotonated phenoxy group (the corresponding peak appears at 1254 cm^{-1} in H_2L). Infrared stretching at 1620 and 1616 cm^{-1} for **1** and **2**, respectively are assigned to coordinated ν(C=N) [60], whereas in free ligand, H_2L, the band appears at higher wave number (1632 cm^{-1}). The $\nu_{(M-N)}$ and $\nu_{(M-O)}$ stretching frequencies are observed at 562 and 434 cm^{-1} for **1**, 576 and 474 cm^{-1} for **2**. The ν(ClO_4) shows band at 1074, 1103 and 1119 cm^{-1} for **1** and 1085, 1107, 1122 cm^{-1} for **2** corresponds to the M–O-(ClO_3) vibration [61] along with a weak shoulder at 625-630 cm^{-1}.

The conductance measurement has been performed in polar solvent, MeCN and nonpolar solvent, nitrobenzene. The molar conductance (Λ_M) data of **1** and **2** are 12 and 19 $S.m^2.mol^{-1}$ in nitrobenzene and 132 and 163 $S.m^2.mol^{-1}$ in acetonitrile

199 respectively which indicate that in nitromethane both complexes appear nonionic
200 where as in acetonitrile they appear 1:1 electrolyte. In both the complexes [Cu(μ-
201 L)Na(ClO_4)(CH_3OH)] (**1**) and [Ni(μ-L)Na(ClO_4)(CH_3OH)] (**2**), ClO_4^- is weakly
202 bonded to sodium center which exhibits solvent polarity dependent coordination. In
203 coordinating polar solvent like, MeCN, the perchlorate group dissociates and shows
204 conductivity while in nitrobenzene the complex is nonconducting, and is supporting to
205 no-dissociation.
206
207 *3.2. The molecular structures of **1** and **2***
208 The molecular structures of [Cu(μ-L)Na(ClO_4)(CH_3OH)] (**1**) (**Figure 1**) and
209 [Ni(μ-L)Na(ClO_4)(CH_3OH)] (**2**) (**Figure 2**) show that the M(II) centre adopts a
210 square-planar geometry with MN_2O_2 coordination (M = Cu(II) (**1**) and Ni(II) (**2**)). The
211 bond lengths are given in **Tables 2** and **3**. In the complexes, the sodium ion is
212 coordinated to two O-methoxy groups, two bridging O-phenolato groups in a pseudo-
213 macrocylic array along with methanol and a perchlorate anion resulting in a six-
214 coordinate O_6-coordination sphere. The Cu(II)---Na(I) separation is 3.4318(14) Å in **1**
215 and the Na(I) and Ni(II) centers in **2** are separated by 3.3793(11) (molecule 1) and
216 3.4289(11) Å (molecule 2). Interestingly, the crystal structure **2** consists of two
217 conformationally related molecules (***Supplementary Material, Fig. S1***) with slightly
218 different orientation among bond parameters (**Figure 2** and **Table 3** record the
219 molecule 2; molecule 1 is given in ***Supplementary Material, Table S1***). The
220 corresponding Ni-N or Ni-O bond distances (molecule 1), [(Ni(1)-N(1), 1.917(2) Å;
221 (Ni(1)-N(2), 1.893(2) Å; Ni(1)-O(3); 1.857(2) Å); Ni(1)-O(2); 1.874(2) Å data are
222 given in ***Supplementary Material, Table S1***] among square planar environment, show
223 higher value in comparing with other molecular unit, [(Ni(2)-N(4), 1.881(2) Å; Ni(2)-

N(3), 1.875(2) Å; Ni(2)-O(11), 1.847(2) Å; Ni(2)-O(12), 1.860(2) Å)] (molecule 2). Similarly, the corresponding Na-O bond distance in six-coordinated arrangement (molecule 1) belongs in the range, 2.313 to 2.403 Å; slightly shorter than in molecule 2, ranging 2.318 to 2.478 Å. While Na-O bond distances differ inversely *i.e.,* the distances are shorter in molecule 1 than molecule 2.

The complex **1** shows one-dimensional polymers through π-π interactions (Cg---Cg separation 3.57 – 3.65 Å) along the crystallographic *b*-axis. Neighboring ribbons are arranged in a herringbone-like motif with a series of edge-to-face (C-H – centroid distances of 2.74 – 3.13 Å) π-interactions to form two-dimensional sheets perpendicular to the crystallographic *ac*-vector (**Figure 3**). Each sheet further interacts through (Me)O-H ⋯O(ClO_3), 2.02(3) Å and ((N=)CH----O(ClO_3), 2.70 Å; and (Phenyl)C–H---O(ClO_3), 2.40-2.70 Å to form a three-dimensional network (**Figure 4**). In **2**, the adjacent molecules pack closely together forming a one-dimensional ribbon-like polymer through a combination of offset face-to-face π-π (phenyl ring---phenyl ring) interactions and phenyl---chelate ring stacking, which propagates along the crystallographic *a*-axis (**Figure 5**). The presence of phenyl-phenyl interactions is indicated by centroid-centroid separations of 3.63 Å, while the phenyl---chelate ring separation is slightly shorter (3.5 Å) [62-64]. The one-dimensional ribbons interact through coordinated methanol – perchlorate, (Me)O-H---O(ClO_3) = 1.979(15) Å (x-1, y, z) and 2.009(14) Å (x+1, y, z)) (**Figure 6a**), whereas the C-H_{phenyl} – perchlorate (2.60-2.70 Å and CH_{imine} – perchlorate (2.60 Å) (**Figure 6b**) hydrogen bonding interaction results in a three-dimensional network.

3.3. Absorption and emission spectra

The UV-vis spectra of the complexes **1** and **2** are recorded in methanol solution

in 200-800 nm and have been compared with free ligand data [45]. The free ligand shows high intense bands (ε, 10^4 mol^{-1} cm^{-1}) at 220, 260, 293 nm which are assigned to π→π* transition and less intense absorptions (ε, 10^3 mol^{-1} cm^{-1}) at 332 and 419 nm are due to n→π* transition. On complexation, the n→π* band in both the complexes are shifted from 332 to 361 and 372 nm for **1** and **2**, respectively. A characteristic feature to copper(II) complex (**1**) is the appearance of broad d–d weak absorption band at 595 nm and [Ni(μ-L)Na(ClO_4)(CH_3OH)] (**2**) shows weak d-d bands at 475 and 590 nm [65,66].

The spectral characteristics are explained with the help of DFT computation of optimized structures of **1** and **2**. The orbital energies along with contributions from the ligands and metal for few MOs are given in **Figure 7** and details are given in the *Supplementary material* (***Figs. S2, S3, S4 and Tables S2, S4*** for ***1*** and ***Fig. S5 and Table S6 for 2***). Both filled and vacant MOs around HOMO and LUMO are constituted mainly by ligand orbitals (L and ClO_4). It is observed that HOMO-5 and other lower energetic occupied MOs carry >80% ClO_4 function in the complex **1** and in LUMO, LUMO+3 to LUMO+5 also have >80% ClO_4 contribution. Similar observation is recorded to [Ni(μ-L)Na(ClO_4)(CH_3OH)] (**2**) in which HOMO-5 to HOMO-8, LUMO, LUMO+4 to LUMO+6 have >45% share of ClO_4. In [Cu(μ-L)Na(ClO_4)(CH_3OH)] (**1**), Cu contributes 12% to HOMO-3, 6% to HOMO-4, 9% to LUMO+7, 59% to LUMO+9. In the complex **2**, Ni contributes irregularly to MOs such as 4% to HOMO-1, 12% to HOMO-2, 90% to HOMO-4, 9% to LUMO+1, 10% to LUMO+2, 32% to LUMO+7 etc. Thus the ligand L and ClO_4 group control over the molecular function and hence the electronic properties of the complexes. Thus, HOMO → LUMO is considered as L(π) → ClO_4(π^*); HOMO-1→LUMO+1 is LLCT (involving ligand L functions) and HOMO→LUMO+6 is designated LMCT (L(π) → Cu(dπ)) transitions in [Cu(μ-

L)Na(ClO_4)(CH_3OH)] (**1**). Same argument for [Ni(μ-L)Na(ClO_4)(CH_3OH)] (**2**) along with an additional HOMO-4→LUMO+2 transition which is (Cu(dπ) → L(π*)) MLCT. The calculated transitions are grouped in **Table 4**. The intensity of these transitions has been assessed from oscillator strength (*f*). In MeCN the longest wavelength band calculated at >659 nm (*f*, 0.0012) for **1** is assigned to L (π) → L(π*) transition followed by high intense transitions at 482 (intra perchlorate CT, IPCT), 407, 372, 353 nm (L(π) → ClO_4(π*)) (detail are given in *Supplementary material* ***Tables S3, S5*** for **1**). In complex **2**, the transitions at 531 nm (*f*, 0.0013) and 461 nm (*f*, 0.0018) are referred to L (π) → L(π*) transitions; the transitions at 380, 366, 354 and 276 are referred to L(π) → ClO_4(π*) transitions (detail are given in *Supplementary material* ***Table S7*** for **2**).

Emission spectroscopy shows that H_2L emits strongly while the complexes, **1** and **2**, are weak emitter. (**Figure 8**). The emission band of H_2L appears at 445 nm upon excitation at 327 nm which is a π→π* emission. The complexes, **1** and **2**, fluoresce weakly at 419 nm when they are excited at 370 nm. Longer wavelength of excitation (MLCT/d-d bands) does not show any emission. The fluorescence quantum yield of the ligand (Φ_L, 0.02) and complexes (Φ_{Ni}, 0.014; Φ_{Cu}, 0.01) were determined using carbazole as reference with known quantum yield value in benzene (Φ_R= 0.42). The fluorescence spectra revealed that fluorescence emission intensity of Schiff bases decreased dramatically on complex formation with transition metal ions which refers to paramagnetic quenching and heavy atom affect. Upon excitation on UV light irradiation (370 nm) ligand dissociation from the complexes (**1** and **2**) may cause weak emission and it is observed indeed (**Figure 8**).

The decay profiles of the ligand and the complexes have been generated and shown in **Figure 9**. The fluorescence life time has been measured for free ligand and the complexes upon excitation at 370 nm. The decay profile of ligand fits with bi-

exponential decay whereas in case of complexes, the nature of fitting is tri-exponential (**Figure 9**). The mean life time ($\tau_f = a_1\tau_1+a_2\tau_2+ a_3\tau_3$ where a_1, a_2 and a_3 are relative amplitudes of decay process) have been calculated to compare excited state stability of the complexes. The life times of both complexes (0.16-0.17 ns) are much lower than the ligand itself (3.16 ns). This indicates that excited states of the complexes are unstable than those of the free ligand. The radioactive and non-radioactive rate constants values are also calculated and they show usual higher k_{nr} (3.08×10^8 (H_2L), 55.05×10^8(1) and 55.05×10^8 (2)) value than the k_r (6.94×10^6, 55.61×10^6(1) and 78.9 x 10^6(2)).

3.4. The EPR spectra

Room temperature (298 K) bulk magnetic measurement accounts diamagnetic property of Ni(II) (d^8) in **2** (μ, 0.14 BM) while one electron subnormal paramagnetism is calculated for Cu(II) (d^9) in **1** (μ, 1.58 BM). The polycrystalline powder of **2** is EPR-silent both at room temperature and 77 K. The behaviour does not change when this is dissolved in organic solvent, such as DMSO, DMF and CH_3OH; the spectrum recorded in DMSO is shown in **Figure 10a**. The explanation of the lack of spectral signals is due to the fact that a square planar Ni(II) is diamagnetic with all the electron coupled (S = 0) [67].

EPR spectra of polycrystalline powder of **1** were recorded at room temperature and 77 K. They do not change significantly with lowering the temperature. No hyperfine coupling constant between the unpaired electron and ^{63,65}Cu nucleus was detected. A half-field signal around 1700 Gauss, indicative a weak coupling between the copper ions, is observed (**Figure 11**). The spectra appear to be tetragonal with $g_{\|}$ =

2.182 and $g_{\perp}$= 2.053 at RT and $g_{\parallel}$ = 2.187 and $g_{\perp}$ = 2.054 at 77 K. The order $g_{\parallel} > g_{\perp} > g_e$ is characteristic of a $d_{x^2-y^2}$ ground state, [68-70] and is consistent with the square planar geometry of **1**.

Anisotropic solution EPR spectra of **1** are typical of mononuclear Cu(II) centres and show a well-resolved hyperfine structure (**Figure 10**, **traces b-c**). The spectra measured in DMSO, DMF and CH_3OH are comparable and the parameters, very similar in the three solvents, are reported in **Table 5**. They were simulated with software WinEPR [46]. The EPR signals show a slight rhombic distortion; for example, in DMSO the following parameters were simulated: g_z = 2.243, A_z = 187 × 10^{-4} cm^{-1}, g_y = 2.069, A_y = 13 × 10^{-4} cm^{-1}, g_x = 2.043, A_x = 11 × 10^{-4} cm^{-1} (**Figure 10**, trace d). The results are consistent with $d_{x^2-y^2}$ ground state and a geometry close to the limit of square planar in solution; the rhombicity may be due to the slight anisotropy along the *x* and *y* axes (for example, the value of the two *trans* angles are slightly different). The spectra of **1** in DMSO, DMF and $CH_3OH$are typical of a Cu(II) species with an equatorial donor set ($O_{phenolic}$, N_{imine}, N_{imine}, $O_{phenolic}$), even if the characteristic super-hyperfine structure is not detected (**Figure 10, traces b-c**). The spectral parameters are in agreement with those reported for square-planar Cu(II) complexes formed by salpn derivatives ((6,6,6)-chelate rings) [28].

3.5. Electrochemistry

The cyclic voltammograms of the complexes in acetonitrile display both oxidative and reductive responses at positive and negative to Ag/AgCl reference electrode (**Figure 12**). At positive potential, one quasi-reversible ($E_{1/2}$,0.69 V(220 mV)) and an irreversible ($E_{pa,}$ 1.05 V) oxidative responses are recorded for complex **2**

along with ligand reduction at -1.12 V (ΔE, 140 mV). First couple may be referred to nickel(II) oxidation, Ni(III)/Ni(II) (**2**) [71]. The complex **1** shows oxidation couple at 0.78 V(ΔE, 160 mV) and 1.18 V (E_{pa}) followed by reduction of chelated ligand at -0.80 V (ΔE, 110 mV). The oxidation couple at lower potential may be referred to Cu(III)/Cu(II) oxidation [72] and irreversible oxidation may be assigned to phenolato→quinonoid oxidation [73]. Reductive response during cathodic scan may arise from ligand (imine) reduction.

Conclusion

Doubly phenoxo-bridged heterodinuclear [Cu(μ-L)Na(ClO_4)(CH_3OH)] (**1**) and [Ni(μ-L)Na(ClO_4)(CH_3OH)] (**2**) complexes, with L being a Schiff base ligand, have been prepared and characterised in solution and the solid state. The crystal structures show that the complexes pack closely into intricate three-dimensional arrays through a variety of intermolecular interactions. The EPR discussion of **1** and systematic discussion of emission spectra with DFT computation of the complexes have been carried out.

Acknowledgements

KD and CS would like to thank to Council of Scientific and Industrial Research and University Grants Commission, New Delhi, India for the grant to carry out the present study. AD would like to thank to The Scientific & Technological Research Council of Turkey (TÜBITAK) for the grant (2221 – Fellowship for Visiting Scientist). JKC acknowledges the support of the Australian Research Council.

Supplementary material

Crystallographic data for structural analysis of **1** and **2** have been deposited to the Cambridge Crystallographic Data Centre, bearing 870813 and 894362. Copies of this information may be obtained free of charge from the Director, CCDC, 12 Union Road, Cambridge, CB2 IEZ, UK (fax: +44-1223-336-033; e-mail deposit@ccdc.cam.ac.uk or http://www.ccdc.cam.ac.uk).

References

[1] S. Biswas, S. Naiya, M.G.B. Drew, A. Ghosh, J. Indian Chem. Soc., 89 (2012) 1317-1322.

[2] K. Bowman-James, A. Bianchi, E. García-Espana, in, Wiley-VCH Verlag GmbH & Co., Weinheim, 2011.

[3] K. Bowman-James, A. Bianchi, E. García-Espana, in, Wiley-VCH, New York, 1997.

[4] A.E. Martell, D.T. Sawyer, Monograph, (1988).

[5] V.K. Peterson, Y. Liu, C.M. Brown, C.J. Kepert, J. Am. Chem. Soc., 128 (2006) 15578-15579.

[6] J.K. Clegg, S.S. Iremonger, M.J. Hayter, P.D. Southon, R.B. MacQuart, M.B. Duriska, P. Jensen, P. Turner, K.A. Jolliffe, C.J. Kepert, G.V. Meehan, L.F. Lindoy, Angew. Chem., Int. Ed., 49 (2010) 1075-1078.

[7] T.G. Appleton, J. Chem. Educ., 54 (1977) 443.

[8] L. Ma, C. Abney, W. Lin, Chem. Soc. Rev., 38 (2009) 1248-1256.

[9] J. Lee, O.K. Farha, J. Roberts, K.A. Scheidt, S.T. Nguyen, J.T. Hupp, Chem. Soc. Rev., 38 (2009) 1450-1459.

[10] M.M. Wanderley, C. Wang, C.-D. Wu, W. Lin, J. Am. Chem. Soc., 134 (2012) 9050-9053.

[11] J.M. Lehn, Supramolecular Chemistry: Concepts and Perspectives, Wiley-VCH, Weinheim, 1995.

[12] W. Meng, B. Breiner, K. Rissanen, J.D. Thoburn, J.K. Clegg, J.R. Nitschke, Angew. Chem., Int. Ed., 50 (2011) 3479-3483.

[13] W.J. Ramsay, T.K. Ronson, J.K. Clegg, J.R. Nitschke, Angew. Chem., Int. Ed., 52 (2013) 13439-13443.

[14] J.K. Clegg, F. Li, K.A. Jolliffe, L.F. Lindoy, G.V. Meehan, S. Parsons, P.A. Tasker, F.J. White, Dalton. Trans., 42 (2013) 14315-14323.

[15] J.K. Clegg, F. Li, L.F. Lindoy, Coord. Chem. Rev., 257 (2013) 2536-2550.

[16] S. Gambarotta, F. Arena, C. Floriani, P.F. Zanazzi, J. Am. Chem. Soc. 104 (1982) 5082-5092.

[17] S. Gambarotta, F. Urso, C. Floriani, A. Chiesi-Villa, C. Guastini, Inorg. Chem. 22 (1983) 3966-3972.

[18] H. Miyasaka, N. Matsumoto, H. Okawa, N. Re, E. Gallo, C. Floriani, J. Am. Chem. Soc. 118 (1996) 981-994.

[19] P. Zanello, S. Tamburini, P.A. Vigato, G.A. Mazzocchin, Coord. Chem. Rev., 77 (1987) 165-273.

[20] P.A. Vigato, S. Tamburini, D.E. Fenton, Coord. Chem. Rev., 106 (1990) 25-170.

[21] R.J. Butcher, E. Sinn, Inorg. Chem., 15 (1976) 1604-1608.

[22] M. Das, S. Chatterjee, S. Chattopadhyay, Inorg. Chem. Commun., 14 (2011) 1337-1340.

[23] P.A. Vigato, S. Tamburini, Coord. Chem. Rev., 248 (2004) 1717-2128.

[24] A. Caneschi, L. Sorace, U. Casellato, P. Tomasin, Pietro A. Vigato, Eur. J. Inorg. Chem., 2004 (2004) 3887-3900.

[25] D. Aguila, L.A. Barrios, O. Roubeau, S.J. Teat, G. Aromi, Chem. Commun., 47 (2011) 707-709.

[26] A. Datta, C.R. Choudhury, P. Talukder, S. Mitra, L. Dahlenburg, T. Matsushita, J. Chem. Res., Synop., (2003) 642-644.

[27] J. Chakraborty, S. Thakurta, B. Samanta, A. Ray, G. Pilet, S.R. Batten, P. Jensen, S. Mitra, Polyhedron, 26 (2007) 5139-5149.

[28] S. Thakurta, J. Chakraborty, G. Rosair, J. Tercero, M.S. El Fallah, E. Garribba, S. Mitra, Inorg. Chem., 47 (2008) 6227-6235.

[29] B.A. Jazdzewski, W.B. Tolman, Coord. Chem. Rev., 200-202 (2000) 633-684.

[30] D.G. Branzea, A. Guerri, O. Fabelo, C. Ruiz-Pérez, L.-M. Chamoreau, C. Sangregorio, A. Caneschi, M. Andruh, Cryst. Growth Des., 8 (2008) 941-949.

[31] S.R. Batten, S.M. Neville, D.R. Turner, Coordination Polymers: Design, Anaylsis and Application, Royal Society of Chemistry, Cambridge, UK, 2009.

[32] P. Bhowmik, H.P. Nayek, M. Corbella, N. Aliaga-Alcalde, S. Chattopadhyay, Dalton. Trans., 40 (2011) 7916-7926.

[33] R. Gheorghe, M. Andruh, J.-P. Costes, B. Donnadieu, M. Schmidtmann, A. Müller, Inorg. Chim. Acta, 360 (2007) 4044-4050.

[34] T. Kajiwara, K. Takahashi, T. Hiraizumi, S. Takaishi, M. Yamashita, Polyhedron, 28 (2009) 1860-1863.

[35] R. Gheorghe, M. Andruh, A. Müller, M. Schmidtmann, Inorg. Chem., 41 (2002) 5314-5316.

[36] A.M. Madalan, N. Avarvari, M. Fourmigue, R. Clerac, L.F. Chibotaru, S. Clima, M. Andruh, Inorg. Chem., 47 (2008) 940-950.

[37] H. Wang, D. Zhang, Z.-H. Ni, X. Li, L. Tian, J. Jiang, Inorg. Chem., 48 (2009) 5946-5956.

[38] P. Bhowmik, S. Jana, P.P. Jana, K. Harms, S. Chattopadhyay, Inorg. Chim. Acta, 390 (2012) 53-60.

[39] P. Bhowmik, S. Jana, P.P. Jana, K. Harms, S. Chattopadhyay, Inorg. Chem. Commun., 18 (2012) 50-56.

[40] D. Cunningham, P. McArdle, M. Mitchell, N. Ní Chonchubhair, M. O'Gara, F. Franceschi, C. Floriani, Inorg. Chem., 39 (2000) 1639-1649.

[41] K. Agapiou, M.L. Mejia, X. Yang, B.J. Holliday, Dalton. Trans., 0 (2009) 4154-4159.

[42] P. Bhowmik, S Chatterjee, S. Chattopadhyay, Polyhedron, 63 (2013) 214-221.

[43] P. Bhowmik, S. Jana, P.P. Jana, K. Harms, S. Chattopadhyay, Inorg. Chem. Commun. 18 (2012) 50-52.

[44] P. P. Chakrabarty, D. Biswas, S. García-Granda, A. D. Jana and S. Saha, Polyhedron 35 (2012) 108-115.

[45] S. Thakurta, J. Chakraborty, G. Rosair, R.J. Butcher, S. Mitra, Inorg. Chim. Acta, 362 (2009) 2828-2836.

[46] Bruker-Franzen Analytic GmbH, Bremen, Germany, 1996.

[47] J.N. Deams, G.A. Crosby, J. Phys. Chem., 75 (1971) 991-1024.

[48] A. Technologies, in, Agilent Technologies Ltd, Yarton, Oxfordshire, UK, 2009-2011.

[49] L.J. Farrugia, J. Appl. Cryst., 32 (1999) 837-838.

[50] G.M. Sheldrick, Acta Cryst. A, 64 (2008) 112-122.

[51] C. Lee, W. Yang, R.G. Parr, Phys. Rev. B 37 (1988) 785-789.

[52] M.J. Frisch, G.W. Trucks, H.B. Schlegel, G.E. Scuseria, M.A. Robb, J.R. Cheeseman,J.A. Montgomery Jr., T. Vreven, K.N. Kudin, J.C. Burant, J.M. Millam, S.S. Iyengar,J. Tomasi, V. Barone, B. Mennucci, M. Cossi, G. Scalmani, N. Rega, G.A.Petersson, H. Nakatsuji, M. Hada, M. Ehara, K. Toyota, R. Fukuda, J. Hasegawa,M. Ishida, T. Nakajima, Y. Honda, O. Kitao, H. Nakai, M. Klene, X. Li, J.E. Knox,H.P. Hratchian, J.B. Cross, V. Bakken, C. Adamo, J. Jaramillo, R. Gomperts, R.E.Stratmann, O. Yazyev, A.J. Austin, R. Cammi, C. Pomelli, J.W. Ochterski, P.Y.Ayala, K. Morokuma, G.A. Voth, P. Salvador, J.J. Dannenberg, V.G. Zakrzewski, S.Dapprich, A.D. Daniels,

M.C. Strain, O. Farkas, D.K. Malick, A.D. Rabuck, K.Raghavachari, J.B. Foresman, J.V. Ortiz, Q. Cui, A.G. Baboul, S. Clifford, J.Cioslowski, B.B. Stefanov, G. Liu, A. Liashenko, P. Piskorz, I. Komaromi, R.L. Martin, D.J. Fox, T. Keith, M.A. Al-Laham, C.Y. Peng, A. Nanayakkara, M. Challacombe, P.M.W. Gill, B. Johnson, W. Chen, M.W. Wong, C. Gonzalez, J.A. Pople, GAUSSIAN 03 Revision D 01, Gaussian Inc., Wallingford, CT, 2004.

[53] GaussView3.0, Gaussian: Pittsburgh, PA.

[54] P.J. Hay, W.R. Wadt, J. Chem. Phys. 82 (1985) 270-283.

[55] R. Bauernschmitt, R. Ahlrichs, Chem. Phys. Lett. 256 (1996) 454-464.

[56] M.K. Casida, C. Jamorski, K.C. Casida, D.R. Salahub, J. Chem. Phys. 108 (1998) 4439-4449.

[57] R.E. Stratmann, G.E. Scuseria, M.J. Frisch, J. Chem. Phys. 109 (1998) 8218-8224.

[58] M. Cossi, N. Rega, G. Scalmani, V. Barone, Comput. Chem. 24 (2003) 669-681.

[59] N.M. O'Boyle, A.L. Tenderholt, K.M. Langner, J. Comput. Chem. 29 (2008) 839-845.

[60] K. Nakamoto, Infrared and Raman Spectra of Inorganic and Coordination , Parts A and B, 5th Ed., John Wiley, New York, 1997.

[61] S. Roy , T. K. Mondal, P. Mitra, C. Sinha, Polyhedron 51 (2013) 27-40.

[62] K.B. Heine, J.K. Clegg, A. Heine, K. Gloe, K. Gloe, T. Henle, G. Bernhard, Z.-L. Cai, J.R. Reimers, L.F. Lindoy, J. Lach, B. Kersting, Inorg. Chem., 50 (2011) 1498-1505.

[63] J.K. Clegg, L.F. Lindoy, B. Moubaraki, K.S. Murray, J.C. McMurtrie, Dalton

Trans., (2004) 2417-2423.

[64] J.K. Clegg, L.F. Lindoy, J.C. McMurtrie, D. Schilter, Dalton Trans., (2006) 3114-3121.

[65] A.B.P. Lever, Inorganic Electronic Spectroscopy, 2nd Ed., Elsevier, New York, 1984.

[66] J. Zubieta, K.D. Karlin, J.C. Hayes, in: K.D. Karlin, J.Zubieta (Eds.), Copper Coordination Chemistry: Biochemical and Inorganic Perspectives, Adenine Press, Albany, NY, 1983, p. 97;21.

[67] F.E. Mabbs, D. Collison, Electron Paramagnetic Resonance of d Transition Metal Compounds, Elsevier, Amsterdam, 1992.

[68] B.J. Hathaway, D. E. Billing, Coord. Chem. Rev. 5 (1970) 143-207.

[69] B.J. Hathaway, Struct. Bond. 57 (1984) 55-118.

[70] E. Garribba, G. Micera, J. Chem. Ed. 83 (2006) 1229-1232.

[71] S. Nandi, D. Bannerjee, J.-S. Wu, T.-H. Lu, A.M.Z. Slawin, J.D. Woollins, J. Ribas, C. Sinha, Eur. J. Inorg. Chem. (2009) 3972-3981.

[72] E. Lamour, S. Routier, J.-L. Bernier, J.-P. Catteau, C. Bailly, H. Vezin, J. Am. Chem. Soc. 121 (1999) 1862-1869.

[73] J.L.N. Xavier, E. Ortega, J.Z. Ferreira1, A.M. Bernardes, V. Pérez-Herranz, Int. J. Electrochem. Sci. 6 (2011) 622-636.

Table 1. Crystallographic data of [Cu(μ-L)Na(ClO_4)(CH_3OH)] (**1**) and [Ni(μ-L)Na(ClO_4)(CH_3OH)] (**2**)

	1	**2**
Empirical formula	$C_{20}H_{24}NaCuN_2O_9Cl$	$C_{20}H_{24}NaNiN_2O_9Cl$
Formula weight	558.39	553.56
Crystal system	Monoclinic	Triclinic
Space group	$P2_1/n$	P-1
a(Å)	16.4736(2)	7.3822(7)
b(Å)	7.5792(10)	14.0384(17)
c(Å)	18.9289(2)	22.8738(18)
$\alpha/^0$	90	98.533(8)
β/°	102.0580(10)	95.345(7)
$\gamma/^0$	90	104.276(9)
$V(Å)^3$	2311.26(5)	2251.0(4)
Z	4	4
D_{calc} (mg m^{-3})	1.605	1.633
μ (mm^{-1})	3.071 (CuK_α)	1.056 (MoK_α)
F(000)	1148	1144
Parameters	331	628
R_1[a] [I > 2σ (I)]	0.0689	0.0484
wR_2[b]	0.2179	0.1016
Goodness of fit	1.068	1.028

[a]$R1 = \Sigma||F_o| - |F_c||/\Sigma|F_o|$ for $F_o > 2\sigma(F_o)$;[b]$wR2 = (\Sigma w(F_o^2 - F_c^2)^2/\Sigma(wF_c^2)^2)^{1/2}$ all reflectionsw=1/[$\sigma^2(F_o^2)$+((0.1511P)^2 + 1.8729P] for **1** andw=1/[$\sigma^2(F_o^2)$+(0.0414P)^2 + 1.4241P] for **2**, respectively, where P=(F_o^2+2F_c^2)/3.

Table 2. Selected bond lengths (Å) and angles (°) for [Cu(μ-L)Na(ClO_4)(CH_3OH)] (**1**).

Cu(1)-N(1B)	1.905(19)	N(2)-Cu(1)-N(1B)	95.0(6)
Cu(1)-O(2)	1.870(2)	O(2)-Cu(1)-O(3)	79.31(10)
Cu(1)-N(2)	1.905(3)	O(3)-Cu(1)-N(2)	92.66(13)
Cu(1)-O(3)	1.860(2)	N(1B)-Cu(1)-O(2)	92.9(6)
Na(1)-O(1)	2.395(3)	Cu(1)-O(3)-Na(1)	110.11(11)
Na(1)-O(3)	2.315(3)	Cu(1)-O(2)-Na(1)	108.97(11)
Na(1)-O(9)	2.378(4)	O(2)-Na(1)-O(3)	61.60(9)
Na(1)-O(5B)	2.469(11)	O(3)-Na(1)-O(4)	68.37(10)
Na(1)-O(2)	2.333(3)	O(2)-Na(1)-O(9)	114.34(13)
Na(1)-O(4)	2.343(3)	O(4)-Na(1)-O(9)	90.35(13)

583 **Table 3.** Selected bond lengths (Å) and angles (°) for [Ni(μ-L)Na(ClO_4)(CH_3OH)]
584 (**2**).
585

586	Ni(2)-N(3)	1.875(2)	N(4)-Ni(2)-N(3)	92.56(9)
587	Ni(2)-O(11)	1.847(2)	N(4)-Ni(2)-O(12)	92.68(9)
588	Ni(2)-N(4)	1.881(2)	O(12)-Ni(2)-O(11)	81.88(8)
589	Ni(2)-O(12)	1.860(2)	O(11)-Ni(2)-N(3)	93.78(9)
590	Na(2)-O(10)	2.423(2)	Na(2)-O(14)	2.371(2)
591	Na(2)-O(12)	2.328(2)	Ni(2)-O(11)-Na(2)	107.92(8)
592	Na(2)-O(13)	2.478(2)	Ni(2)-O(12)-Na(2)	107.06(8)
593	Na(2)-O(11)	2.318(2)	O(12)-Na(2)-O(11)	63.04(7)
594	Na(2)-O(18)	2.326(2)		
595	Na(2)---Ni(2)	3.3793(11)		

596
597
598
599
600
601
602
603
604
605
606
607

608 **Table 4**. Assignment of spectral transitions of the complexes following TD-DFT

609 computation

Excitation energy (eV)	λ (nm)	f	Key Transitions	Character
[Cu(μ-L)Na(MeOH)(ClO_4)] (**1**)				
1.8807	659.24	0.0012	(51%) HOMO→LUMO+1	LLCT
2.1514	576.31	0.0019	(98%) HOMO-1→LUMO+1	LLCT
2.2676	546.75	0.0053	(40%) HOMO-7→LUMO	IPCT
2.5702	482.39	0.0145	(49%) HOMO-7→LUMO	IPCT
3.0424	407.51	0.0660	(52%) HOMO→LUMO+5	LPCT
3.3248	372.91	0.0118	(52%) HOMO-1→LUMO+4	LPCT
3.3823	366.57	0.0592	(66%) HOMO-1→LUMO+5	LPCT
3.5051	353.72	0.0384	(66%) HOMO-1→LUMO+6	LPCT
3.7816	327.86	0.0050	(65%) HOMO-7→LUMO+1	PLCT
[Ni(μ-L)Na(MeOH)(ClO_4)] (**2**)				
2.3322	531.62	0.0013	(72%) HOMO-1→LUMO+1	LLCT
2.6854	461.70	0.0018	(95%) HOMO-1→LUMO+2	LLCT
3.2601	380.31	0.0778	(37%) HOMO→LUMO+5	LPCT
3.3847	366.31	0.0217	(39%) HOMO-1→LUMO+4	LPCT
3.4980	354.45	0.0633	(37%) HOMO-1→LUMO+5	LPCT
3.8413	322.77	0.0042	(20%) HOMO→LUMO+6	LMCT
4.4824	276.60	0.1150	(32%) HOMO-4→LUMO+5	LPCT
5.0094	247.50	0.0030	(24%) HOMO-9→LUMO+1	PLCT
5.2612	235.66	0.0115	(37%) HOMO→LUMO+8	ILCT

610

611 LLCT (L(π) → L(π*)); IPCT (intra perchlorate charge transfer); LPCT (ligand

612 toperchlorate charge transfer); LMCT (L(π)→Cu(dπ); PLCT (perchlorate to ligand

613 charge transfer); ILCT (intra ligand charge transfer)

614

615 **Table 5**. EPR parameters of **1** in different solvents.

Species	Solvent	g_x	A_x / 10^{-4} cm^{-1}	g_y	A_y / 10^{-4} cm^{-1}	g_z	A_z / 10^{-4} cm^{-1}
2	DMSO	2.037	11	2.069	13	2.243	187
2	DMF	2.037	11	2.070	12	2.243	187
2	CH_3OH	2.036	12	2.069	13	2.243	188

616

617

618

619

620

621

622

623

624

625

626

627

628

629

630

631

632

633

634

635

636

Figure captions

Fig. 1. ORTEP representation of **1** shown with 50 % probability ellipsoids. Regions of disorder omitted for clarity.

Fig. 2. ORTEP representation of one of the two chemically identical, but crystallographically independent molecules in **2** shown with 50% probability ellipsoids.

Fig. 3. View of the **1** down the crystallographic *ac*-vector showing part of the two-dimensional layers formed through herringbone-like arrangements of one-dimensional chains. Chains are colored alternately.

Fig. 4. View of the **1** down the crystallographic *ac*-diagonal. Each layer interacts through a series of hydrogen bonds (not shown).

Fig. 5. Schematic representation of part of the one-dimensional ribbon-like polymer formed through π-π interactions in **2**. Arrows indicate π-π interactions.

Fig. 6. Schematic representation of parts of the formal (a) and informal (b) hydrogen bond interactions in **2**. Dashed lines indicate hydrogen bonds.

Fig. 7. Surface plots of some MOs (HOMO-1, HOMO, LUMO and LUMO+1) of $[Cu(L)Na(MeOH)(ClO_4)]$ (**1**) and $[Ni(L)Na(MeOH)(ClO_4)]$ (**2**)

Fig. 8. . Emission spectra of (a) H_2L (in DMF), (b) complex **2** (in MeOH) and (c) complex **1** (in DCM).

Fig. 9. Exponential decay profile (•) and fitting curve (—) of (a) H_2L (b) complex **1**(in DCM) and (c) complex **2** (in MeOH). Excitation is carried out at 370 nm.

Fig. 10. Anisotropic X-band EPR spectra of: (a) **2** in DMF, (b) **1** in DMF, (c) **1** in DMSO and (d) simulated spectrum of **1** in DMSO. Diphenylpicrylhydrazyl (dpph) is the standard field marker (g = 2.0036). The spectra in the traces (a)-(c) were recorded

with the same instrumental gain. Inset figure shows spin density of [Cu(μ-L)Na(MeOH)(ClO_4)] considering optimized structure.

Fig. 11. X-band EPR spectra of the polycrystalline complex **1** at (a) RT and (b) 77 K. Diphenylpicrylhydrazyl (dpph) is the standard field marker (g = 2.0036).

Fig. 12. Cyclic voltammogram of complexes **1** and **2** in MeCN using Pt-disk working electrode, Pt-wire auxiliary and SCE reference electrode in presence of [n-Bu_4N](ClO_4) supporting electrolyte at 50 mV S^{-1} scan rate at 300K.

Figure 1.

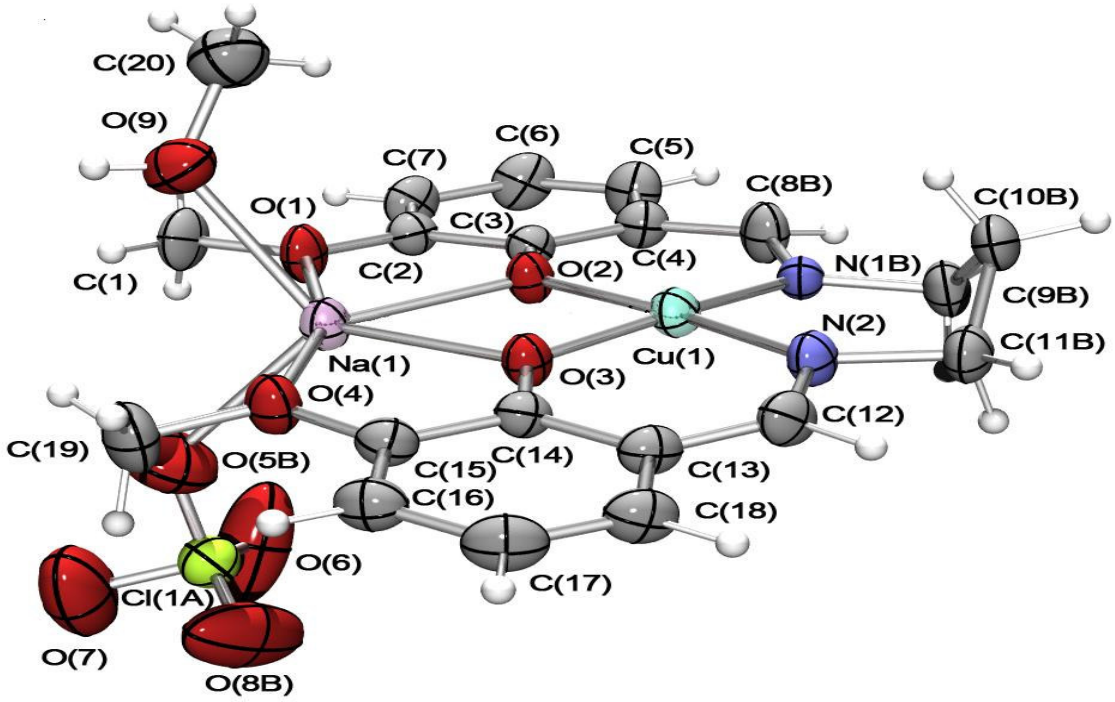

703 **Figure 2.**

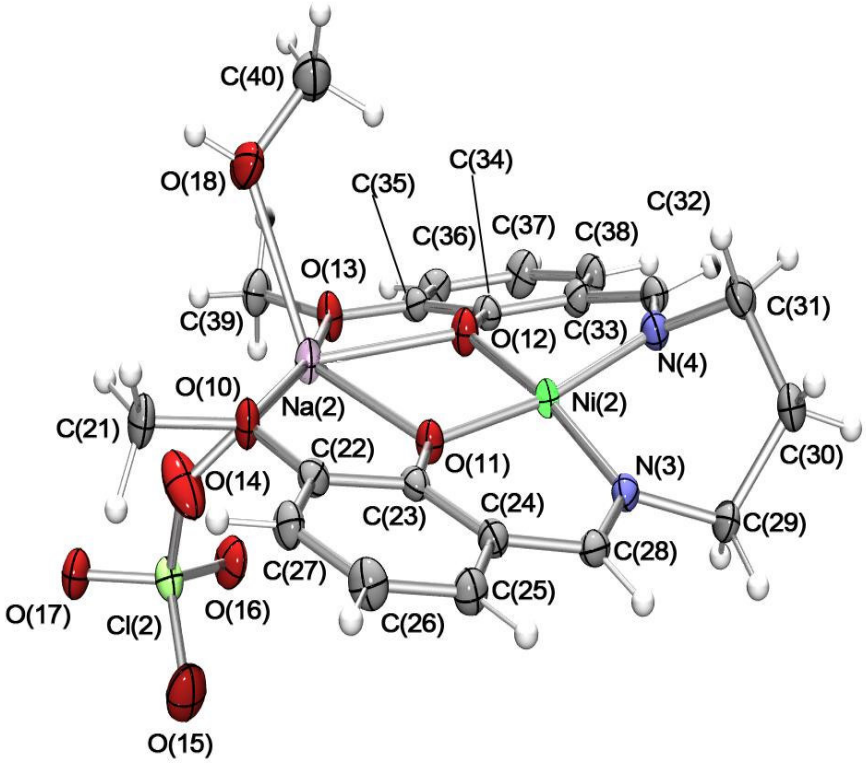

704

705

706 **Figure 3.**

707

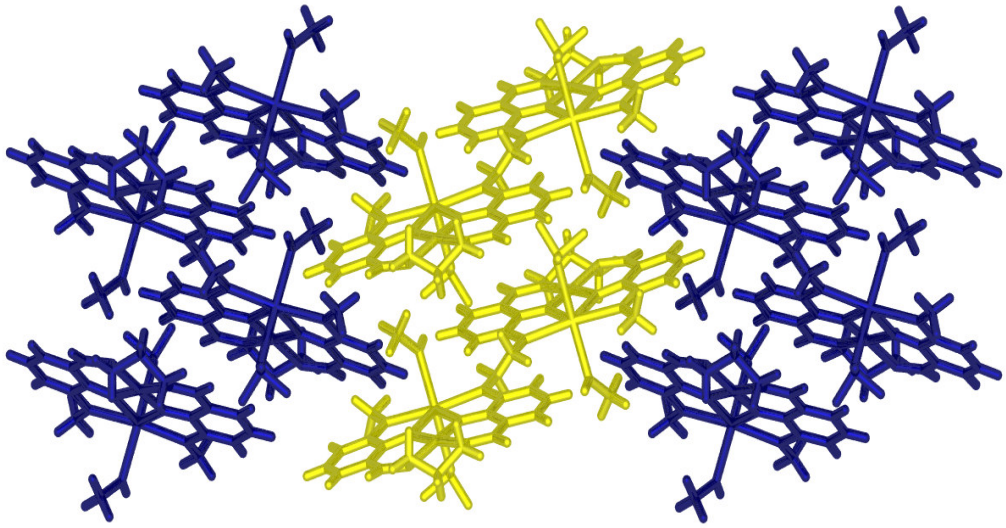

708

709

710 **Figure 4.**

711

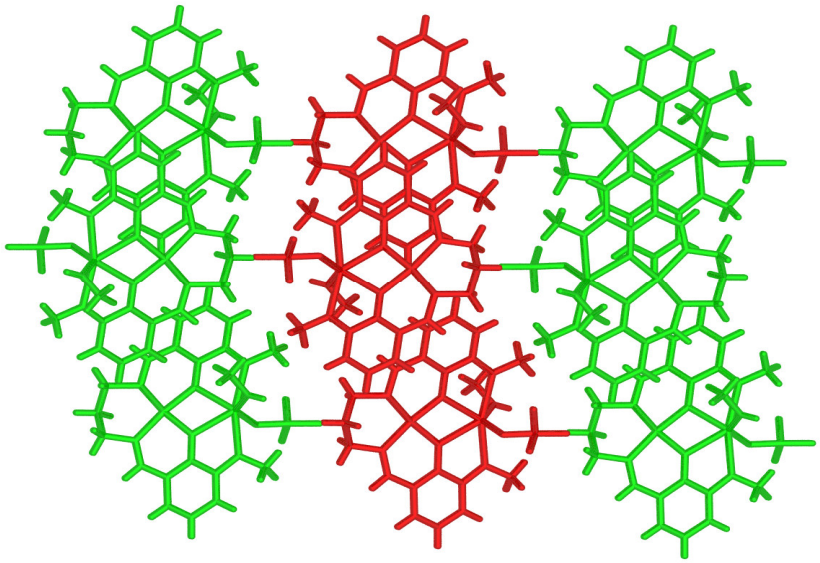

712

713

714 **Figure 5.**

715

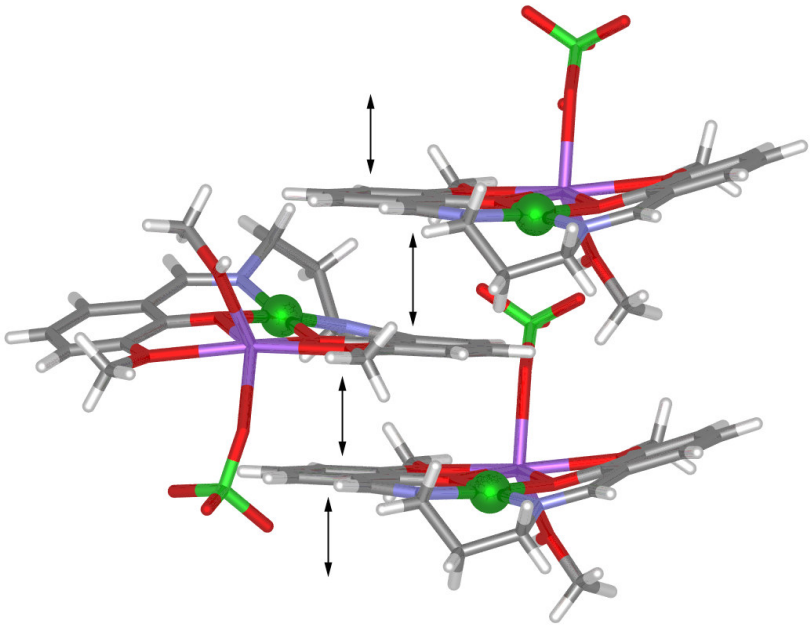

716

717

718 **Figure 6.**

719

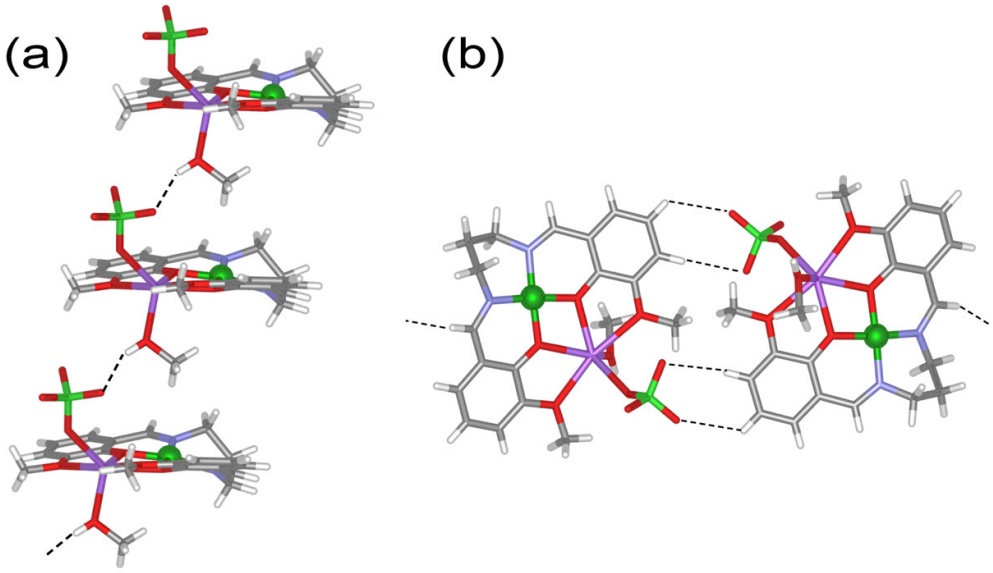

720

721

722

723

724

725

726

727

728

729

730

731

732

733

734

735

736

737

738

739

740 **Figure 7.**

741

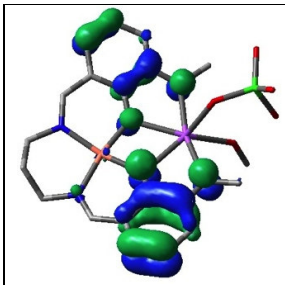	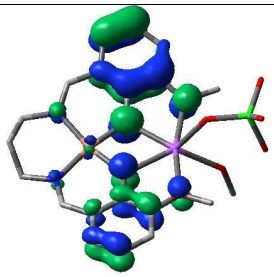	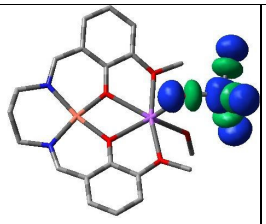	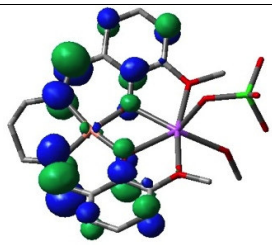
HOMO-1, E = -5.87 eV; Cu, 2%; L, 98%	HOMO, E = -5.66 eV; L, 99%	LUMO, E = -3.32 eV; ClO_4, 98%	LUMO+1, E = -2.27 eV; Cu, 2%, L, 98%
[Cu(L)Na(MeOH)(ClO_4)] (**1**)			
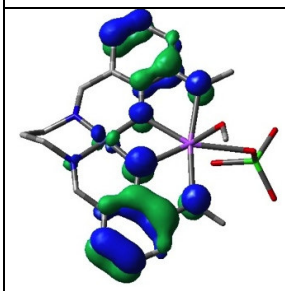	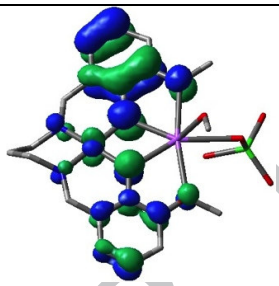	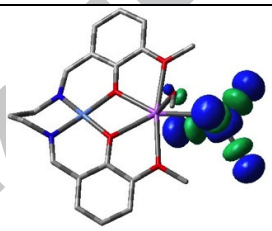	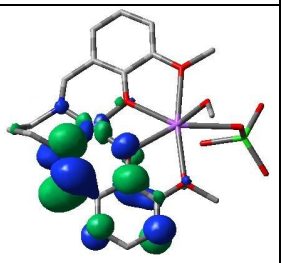
HOMO-1, E = -5.83 eV; Ni, 4%; L, 96%	HOMO: E = -5.56 eV; Ni, 7%; L, 93%	LUMO,E = -3.35 eV; ClO_4, 97%	LUMO+1, E = -2.22 eV; Ni, 9%; L, 91%
[Ni(L)Na(MeOH)(ClO_4)] (**2**)			

742

743

744

745

746

747

748

749

750

751

752

753 **Figure 8.**

754

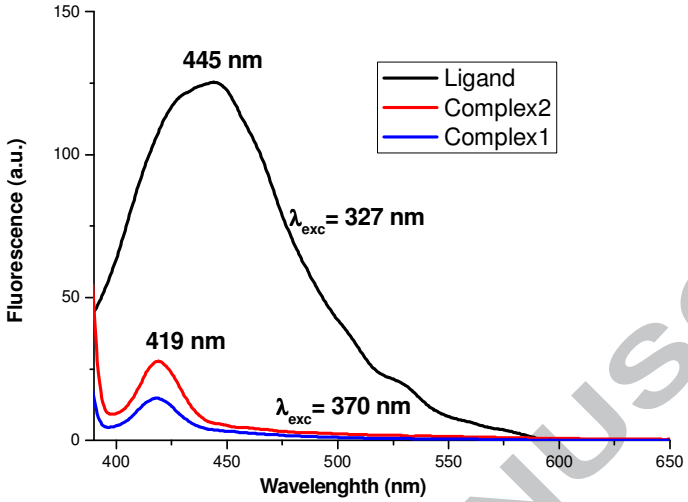

755

756

757 **Figure 9.**

758

759

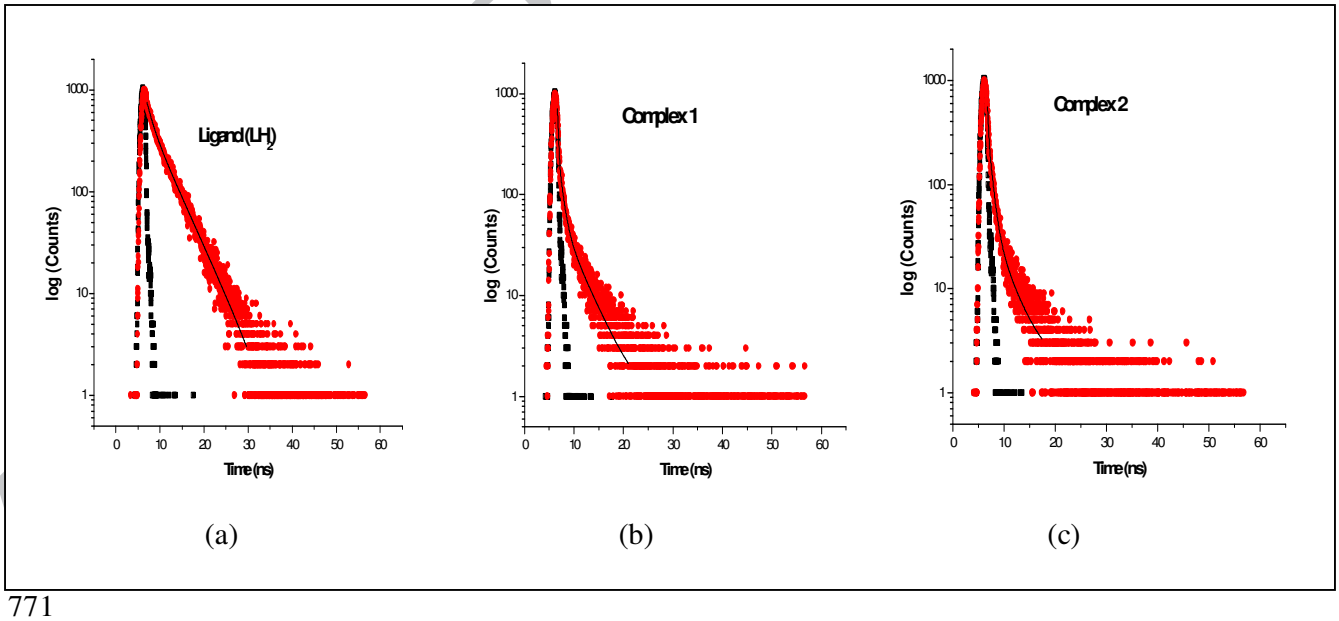

771

772

773

774

Figure 10.

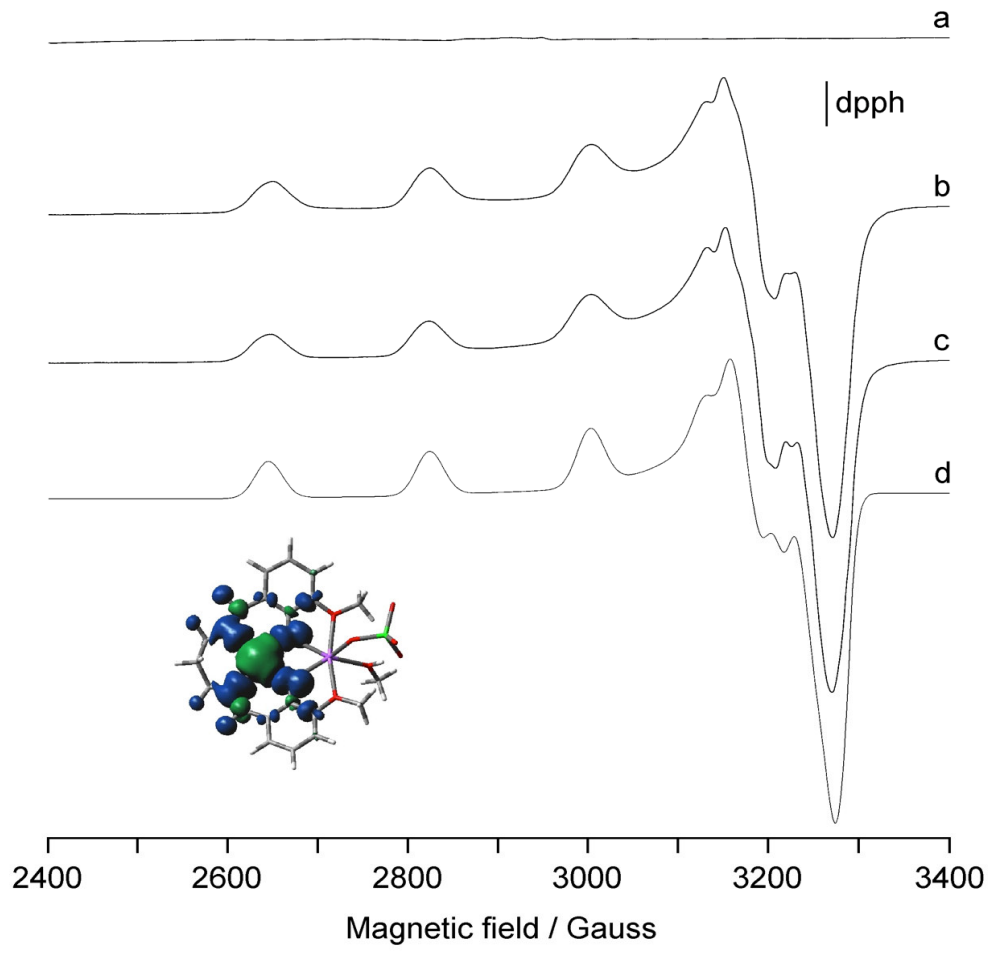

Figure 11.

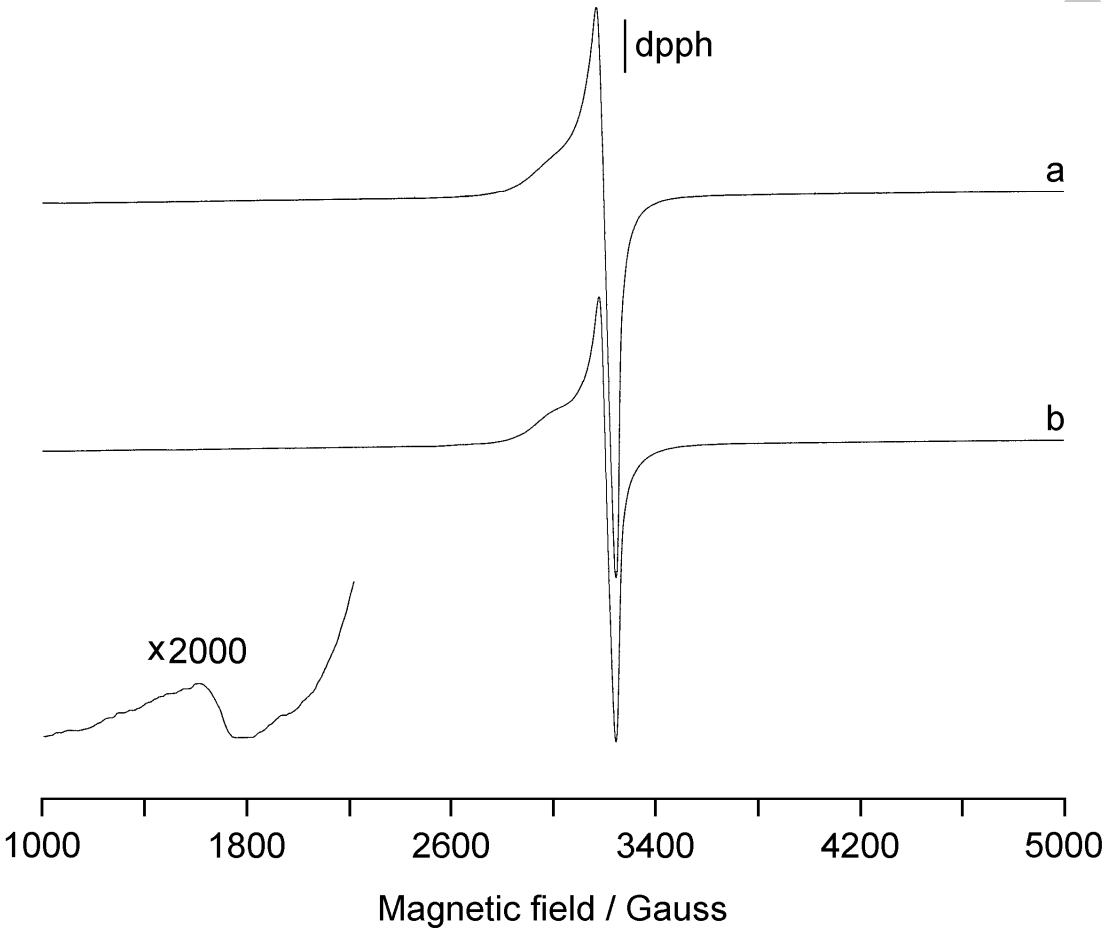

824

825 **Figure 12.**

826

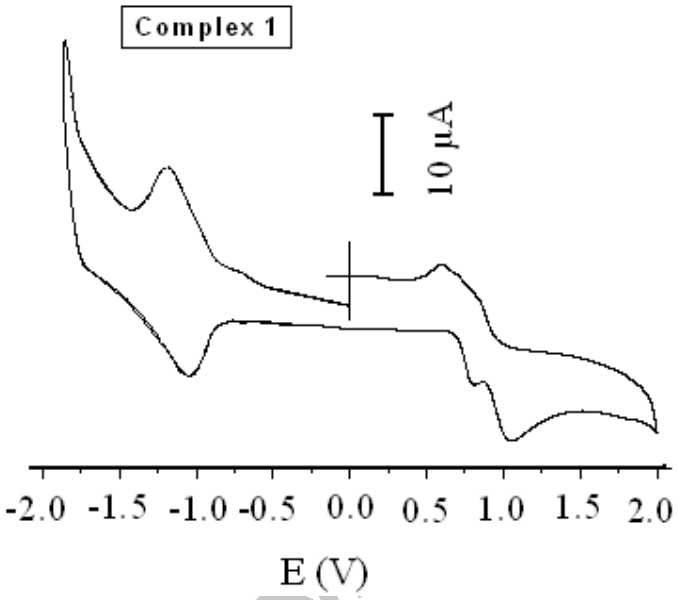

827

828

829

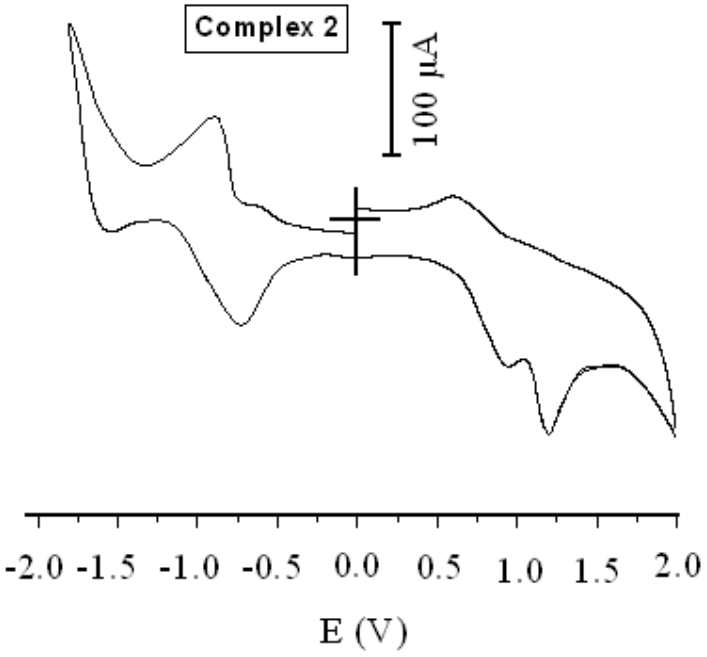

830

831

832

GRAPHICAL ABSTRACT

Doubly phenoxo-bridged M-Na (M = Cu(II), Ni(II)) complexes of tetradentate Schiff base: Structure, photoluminescence, EPR, electrochemical studies and DFT computation

Kuheli Das, Amitabha Datta* Suman Roy, Jack K. Clegg, Eugenio Garribba, Chittaranjan Sinha* Hulya Kara

N,*N*'-Bis(3-methoxysalicylidenimino)-1,3-diaminopropane [**LH_2** = $C_6H_3(OMe)(OH)–CH=N–(CH_2)_3–N=CH–C_6H_3(OMe)(OH)$] is a tetradentate N_2O_2 ligand forms heterometallic complexes [M(μ-**L**)Na(ClO_4)(CH_3OH)] (M = Cu (**1**), Ni(**2**)). Single-crystal X-ray diffraction studies reveal phenolato bridged, M(μ-L)Na, unit. The Cu(II)---Na(I) separation is 3.4318(14) Å in **1** and the Na(I) and Ni(II) centers in complex **2** are separated by 3.3793(11) (molecule 1) and 3.4289(11) Å (molecule 2). The complexes show M(III)/M(II) redox couple alongwith phenolato oxidation. Both the compounds were characterized by elemental analysis, IR, UV-vis, EPR, photoluminescence and DFT computation study.

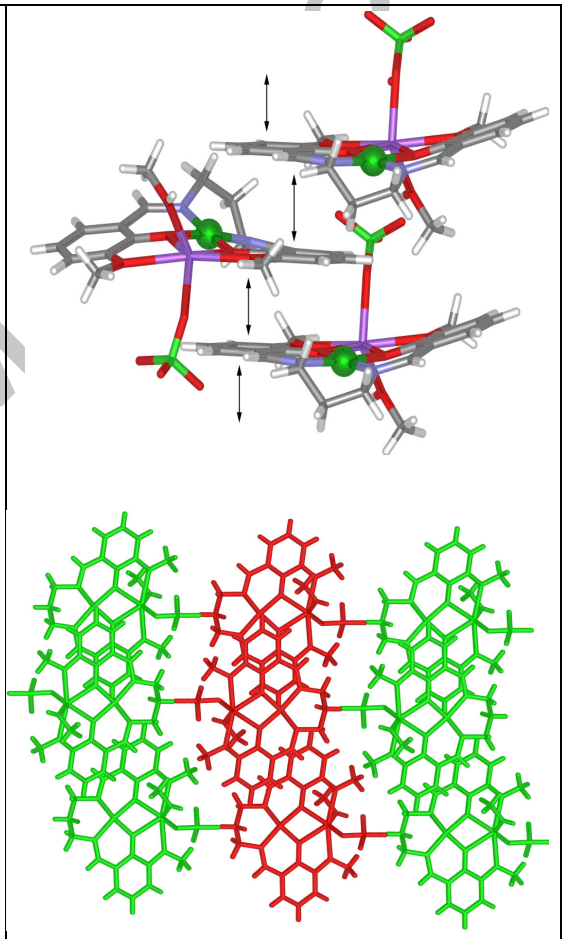

PICTORIAL ABSTRACT

Doubly phenoxo-bridged M-Na (M = Cu(II), Ni(II)) complexes of tetradentate Schiff base precursor: Structure, photoluminescence, EPR, electrochemical studies and DFT computation

Kuheli Das, Suman Roy, Jack K. Clegg, Eugenio Garribba , Chittaranjan Sinha*, Amitabha Datta*

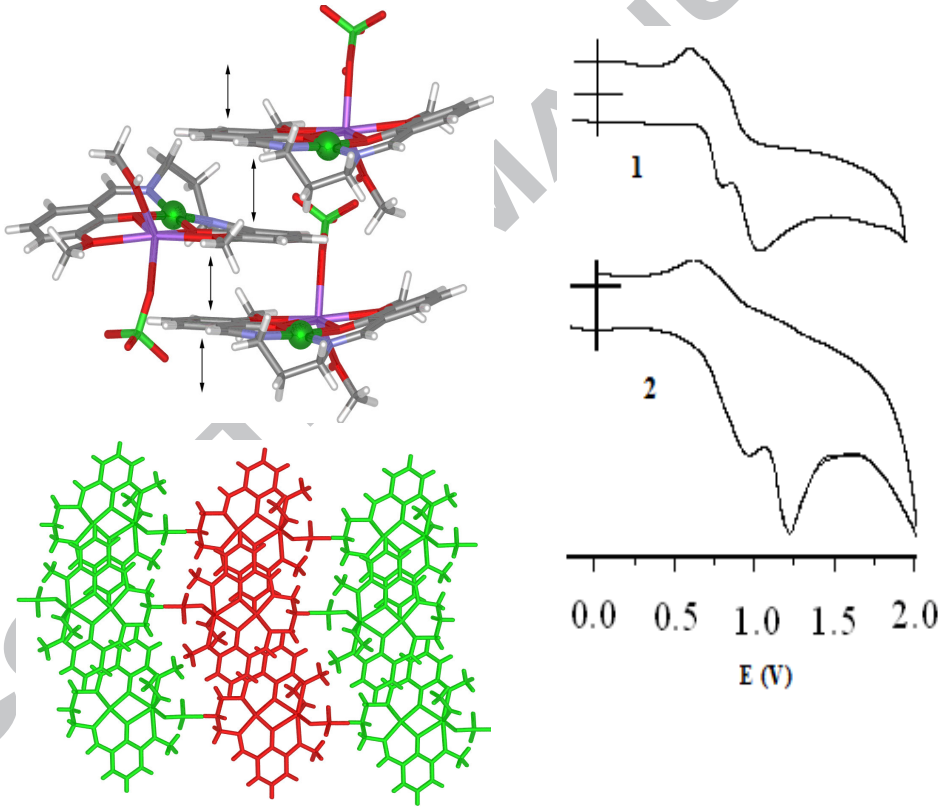

HIGHLIGHTS

Doubly phenoxo-bridged M-Na (M = Cu(II), Ni(II)) complexes of tetradentate Schiff base: Structure, photoluminescence, EPR, electrochemical studies and DFT computation

Kuheli Das, Amitabha Datta* Suman Roy, Jack K. Clegg, Eugenio Garribba, Chittaranjan Sinha* Hulya Kara

- ► *N*,*N*'-bis(3-methoxysalicylidenimino)-1,3-diaminopropane.
- ► Phenoxobridging heterometallic Cu(II)/Ni(II)-Na complexes.
- ► X-ray structures, absorption and emission spectra, EPR characterisation.
- ► Ni(III)/Ni(II) and Cu(III)/Cu(II), phenoxide oxidation.
- ► DFT and TD-DFT computation.

PICTORIAL ABSTRACT

Doubly phenoxo-bridged M-Na (M = Cu(II), Ni(II)) complexes of tetradentate Schiff base: Structure, photoluminescence, EPR, electrochemical studies and DFT computation

Kuheli Das, Amitabha Datta* Suman Roy, Jack K. Clegg, Eugenio Garribba, Chittaranjan Sinha* Hulya Kara